UDC 520.6.05 DOI: 10.18698/0236-3933-2021-4-139-151

METHOD FOR CALCULATING THE OFFNER COMPACT-SIZE SPECTROMETER

V.I. Zavarzin zavarzin@bmstu.ru
I.M. Zaitsev zajcev06061997@mail.ru
S.V. Yakubovskiy yakubovskiystas@mail.ru

Bauman Moscow State Technical University, Moscow, Russian Federation

Abstract

Significant advances in development of the optical wavelength range require high-quality optical systems to create optoelectronic equipment on their basis characterized by high speed and information capacity. A method for calculating a compact-size Offner spectrometer was developed having the advantages of its compactness, maintaining high optical characteristics and having relatively low cost in comparison with the large-size equipment. The method is based on using the Rowland circles and the coma and astigmatism correction in the image plane. Analytical expressions were obtained making it possible to calculate design parameters of the spectrometer optical scheme. Two examples of calculating optical systems for visible and infrared ranges were considered. Calculated systems were simulated in the Zemax software program. To evaluate the synthesized optical models image quality, the confusion spot radius in the image plane was used. It is demonstrated that the confusion spot radius value does not exceed the value of the radiation receiver pixel size in the considered spectral ranges. Optimization was carried out for the IR spectrometer according to overall dimensions in order to improve the design manufacturability. It is shown that the principles laid down in the method development are effective, and the method itself could be used in design and development of new small-size hyperspectral optoelectronic equipment

Keywords

Compact-size spectrometer, Offner scheme, wide spectral range

Received 11.05.2021
Accepted 08.06.2021

Introduction. Significant progress was achieved nowadays in the optical wavelength range development. New sources and optical radiation receivers, and high-quality optical systems were developed. Optoelectronic equipment is being created on their basis characterized by high speed and information capacity, which expands and increases the role of optical research in studying

the surrounding world. More and more, optical methods are introduced into the Earth remote sensing. Special place in the Earth remote sensing is occupied by optical equipment and methods of contactless study of the surveyed object characteristics. To obtain not only qualitative, but also quantitative information about the registered object, spectral analysis is used by hyperspectral equipment registering a spectral interval of electromagnetic radiation dozens of times wider than the human eye. Such equipment is often having large dimensions and weight, which technically complicates its use. But, in contrast to large-size optoelectronic equipment, compact-size devices have minor mass and size, due to which design, production and further maintenance cycle are carried out with lower costs in finance and resources once again emphasizing relevance, prospects and efficiency of using the compact-size devices [1].

Reliability of the optoelectronic equipment operation in the Earth remote sensing requires stability in space and time, which originates a number of severe restrictions regarding design and maintenance of technical characteristics at high-level during operation.

Problem statement. General trend in the optoelectronic equipment development lies in increasing optical characteristics and resolution, broadening the spectral range with a decrease in overall dimensions, weight and radiation losses. This places high demands to accuracy and quality of the design work. From the point of view of concept and methods, this currently implies calculation of optical systems of the Earth remote sensing optoelectronic equipment with severe restrictions on dimensions and weight in conditions of import substitution with limited financial and material resources.

Classical schemes and methods could no longer fully meet the ever-increasing requirements to optical system of the Earth remote sensing optoelectronic equipment. Therefore, creation of the compact-size multifunctional optoelectronic equipment became a priority. Creation of such equipment is possible on the basis of new structural and optical materials, fundamentally new optical systems, for example, such as the mirror lens with a minor number of surfaces. The Offner scheme is the most promising among all possible schemes for constructing spectrometers, because of its simplicity, minor dimensions and high optical characteristics in a wide spectral range. Using such schemes would provide possibility to register radiation in a wide spectral range from ultraviolet to the far IR range, including hyperspectral imaging with the number of spectral channels up to several hundred. Possibility to achieve high image quality in a place convenient for installing complex equipment for recording and analyzing images is of particular importance in such systems. Their design should provide reliable image protection from parasitic illumination.

Work objective is to elaborate methodology for designing the compact-size spectrometer optical system making it possible to optimize design solution and obtain high-quality image close to the diffraction. The confusion spot radius in the image plane is used as a criterion in the image quality evaluation. With ideal optical system and dispersing device, it is the confusion spot size that determines spectral and spatial resolution.

Spectrometer optical scheme calculation. Optical system of the spectrometer consists of lens and dispersive component, which role could be played by various elements in the form of a prism/set of prisms and a diffraction grating. In order to reduce the system overall size and minimize the chromatic aberration effect on image quality in selecting the lens components, mirrors are generally preferred. Spectrometer design built according to the Offner scheme (Fig. 1) is, in the general case, a three-mirror system with a convex diffraction grating on the second mirror, where the aperture diaphragm is also installed.

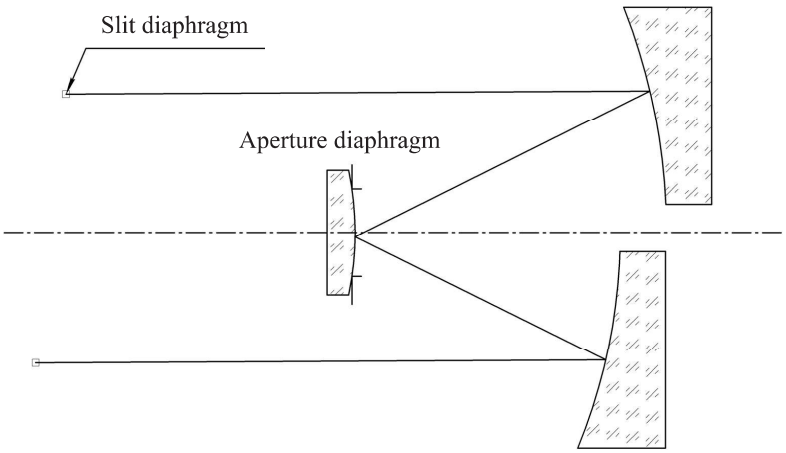

Fig. 1. Offner spectrometer optical scheme

Calculation is based on using the Rowland circles [2–8] and the corresponding condition, under which it is sufficient to obtain image without a coma that the object point *O* (entrance slit) lies on the first Rowland circle, and at the same time the *I* final and intermediate images of the *O* point should lay on the Rowland circles of each scheme component (Fig. 2). Replacing the first concave mirror by the two separate ones with all the spherical elements installed on the Rowland circles with the *z* axis intersection point leads to a decrease in astigmatism. Point *C* is the circles' intersection point at the *z*-axis.

In Fig. 2 point *I* and angle φ' are the points of meridional image and the meridional angle.

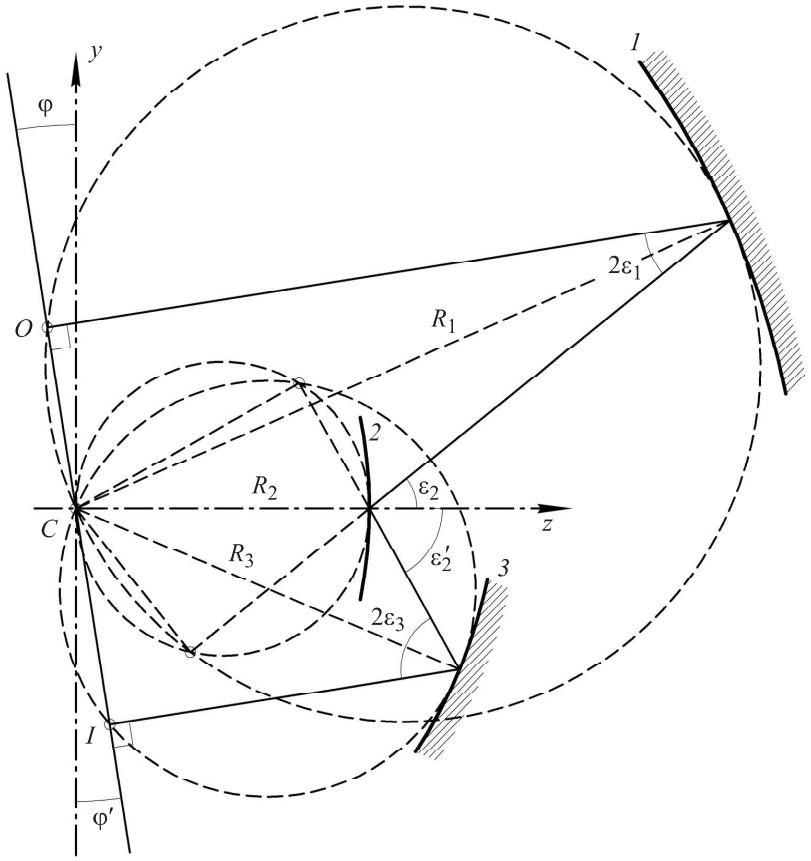

Fig. 2. Rowland circles formed by three spectrometer scheme components

The designed spectral device should operate in the wavelength range from λ_1 до λ_2, where the λ_0 main wavelength is selected as the average for this range or being correspondent to the maximum sensitivity of a radiation receiver. Then, the difference between extreme wavelengths of the operating spectral range is

$$\Delta\lambda = \lambda_2 - \lambda_1. \tag{1}$$

Let the required spectral resolution of the $d\lambda$ device be given. Hence the number of channels operating in the radiation receiver is determined as

$$N_c = \frac{\Delta\lambda}{d\lambda}. \tag{2}$$

Resolution element (pixel) size of the radiation receiver is δ. And the size of the spectral image is

$$h_{sp} = N_c \delta. \tag{3}$$

Calculation is carried out for the $k = -1$ diffraction order, since in this case the dispersed radiation wave contains most of the light energy [2]. The main beam incidence angle on the third surface is ε_3. It is recommended to consider the angle value of $0 < \varepsilon_3 < 25°$ [3], so that the grating could possess up to 90 % of energy concentration in a certain spectrum order (–1). The diffraction grating groove frequency is denoted by m (lines/mm).

Let us use the anastigmatism condition to find the angle of image position deviation (meridional angle) from the original y-axis (object plane), thereby ensuring that the astigmatism value is at least of the second order of the wavelength [3]:

$$\frac{\sin^3\varepsilon_3}{\cos\varepsilon_3} + \operatorname{tg}\varphi' - \operatorname{tg}\varepsilon_3 \cos 2\varepsilon_3 \operatorname{tg}^2\varphi' + \frac{1 + 2\sin^2\varepsilon_3}{2}\operatorname{tg}^3\varphi' = 0. \tag{4}$$

Having solved the cubic equation for φ', desired value of the image position deviation angle is obtained from the original axis.

Main beam reflection angle from the second surface is in the following form:

$$\varepsilon_2' = \varphi' + 2\varepsilon_3. \tag{5}$$

The second mirror radius is determined by the formula

$$R_2 = \frac{h_{\text{sp}}}{k\, m\, \Delta\lambda}. \tag{6}$$

The third surface (third mirror) radius is found as

$$R_3 = \frac{R_2 \sin\varepsilon_2'}{\sin\varepsilon_3}. \tag{7}$$

Distance CI from the circles' intersection point to the image point could be determined in two ways from formula (7), and due to the φ' angle smallness, it could be considered equal to the y' image position on the y-axis:

$$CI = R_2 \sin\varepsilon_2' = R_3 \sin\varepsilon_3 \cong y'. \tag{8}$$

Main beam incidence angle on the second surface is defined as

$$\varepsilon_2 = k\,\lambda\, m - \sin\varepsilon_2'. \tag{9}$$

Object position deviation angle from the original axis is equal to

$$\varphi = \operatorname{arctg}\left(\frac{-\sin\varepsilon_2' \operatorname{tg}\varphi'}{\sin\varepsilon_2}\right). \tag{10}$$

Main beam incidence angle on the first surface is calculated as

$$\varepsilon_1 = \frac{\varphi - \varepsilon_2}{2}. \tag{11}$$

First surface (first mirror) radius is in the form

$$R_1 = -\frac{R_2 \sin \varepsilon_2}{\sin \varepsilon_1}. \tag{12}$$

Object position by analogy with (8) could be determined in two ways from formula (12), and it could be considered equal to the *CO* distance from the circles' intersection point to the object point:

$$CO = -R_1 \sin \varepsilon_1 = R_2 \sin \varepsilon_2 \cong y. \tag{13}$$

Next let us determine position of mirrors relative to each other through the axial distances. Distance from the object plane (y-axis) to the first mirror taking into account the φ inclination angle is calculated by the formula

$$d_0 = \left|R_1 \cos \varepsilon_1\right| - \left|CO \operatorname{tg} \varphi\right|. \tag{14}$$

Distance between the first and the second mirrors is the radii difference:

$$d_1 = R_1 - R_2. \tag{15}$$

Distance between the second and the third mirrors by analogy with (15) is

$$d_2 = R_2 - R_3. \tag{16}$$

Calculation according to formulas (1)–(16) completely determines the Offner spectrometer design parameters.

Example 1. Design of Offner spectrometer operating in the visible range. Initial design data are as follows: spectral range is $\lambda_1 - \lambda_2$ (0.4–0.8 μm); radiation receiver resolution element size δ = 6.5 μm; required spectral resolution $d\lambda$ = 5 nm; F-number K = 10.

According to formulas (1)–(16), let us calculate design parameters of the Offner spectrometer optical scheme (Table 1). Design parameters obtained are used for simulation in the Zemax analysis and optical systems design software package [9]. Note that the number of m lines of the diffraction grating in the Zemax program is set in lines/μm. In this case m = 0.1 lines/μm.

Simulation results shown in Fig. 3 make it possible to estimate the root-mean-square value of the confusion spot points' radius in the image plane for the fundamental wavelength λ_0 = 0.6 μm and at the following field points: –3.745, –1.872 mm and 0. Coordinates are set in such a way as to ensure possi-

bility to evaluate the confusion spot points' size along the entire length of the radiation receiver line equal to 7.488 mm. Slit width is taken equal to the pixel size. Object position is $y = 5.513$ mm. The size of the Airy disc shown in Fig. 3 in the form of a circle is 7.329 μm.

Table 1

Design parameters of a spectrometer operating in the visible range

Surface	Radius *R*, mm	Thickness *R*, mm	Optical material
Object plane	∞	26.009	–
Concave mirror 1	–26.575	–13.575	Mirror
Aperture diaphragm. Diffraction grating	–13.000	11.330	
Concave mirror 3	–24.330	–24.897	
Image plane	∞	–	–

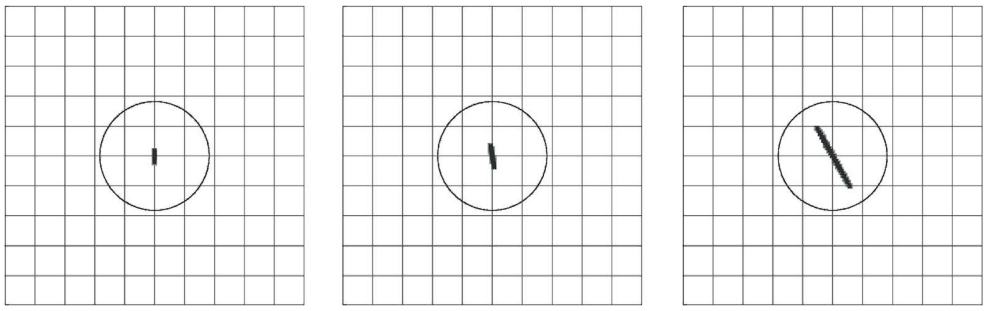

a *b* *c*

Fig. 3. Confusion spot points in the image plane of the 0.6 μm wavelength: *a* are O (0; 5.513), I (0; –4.732 mm), RMSV-rad (0.454 μm); *b* are O (–1.872; 5.513), I (1.872 mm; –4.731 mm), RMSV-rad (0.85 μm); *c* are O (–3.745; 5.513), I (3.741 mm; –4.726 mm); (RMSV-rad (2.451 μm) O is object (slit); I is image (on the matrix); RMSV-rad is root-mean-square value of the confusion spot radius; reference grid scale 40 μm)

It follows from Fig. 3 that the maximum root-mean-square value of the confusion spot radius is 2.451 μm. It may be concluded from this that the confusion spot point size in the image plane is not exceeding the pixel size of the radiation receiver matrix ($2 \cdot 2.451$ μm < 6.5 μm), i.e., there is no loss in the useful light signal (excluding diffraction phenomena), which confirms correct design of the Offner spectrometer operating in the visible spectral range in accordance with the initial requirements.

After simulating the spectrometer, let us evaluate its overall dimensions. To do this, the Zemax program will be used. Based on Zemax data obtained, the total system length is 27.1422 mm; maximum light diameter is 16.3543 mm.

Calculated spectrometer demonstrated satisfactory compliance with the specified conditions for correcting coma and astigmatism, which values are –0.0001211 mm and –0.02575 mm (maximum field).

Example 2. Design of Offner spectrometer operating in the near IR range. Initial design data are as follows: near infrared range $\lambda_1 - \lambda_2$ (0.85–1.70 μm), where the fundamental wavelength is selected equal to $\lambda_0 = 1.275$ μm; required spectral resolution of the device $d\lambda = 10$ nm; receiver resolution element (matrix pixel) size $\delta = 20$ μm; line frequency $m = 0.1$ lines/μm; F-number $K = 10$.

In connection with complexity of the IR devices control and adjustment operations [10, 11] caused by peculiarities of the light rays invisible to the human eye passage through optical elements, it makes sense to simplify the optical circuit, which includes reducing the number of its components, eliminating all possible tilts thereof and maintaining symmetry relative to the optical axis. This becomes possible, if the first and the third mirrors of the Offner spectrometer are made in the form of a common element, i.e., the main mirror, which is ensured by equality of the R_1 and R_3 radii. Then, positions of the spectrometer first and third mirrors would coincide. It follows from formulas (7) and (12) that this equality is attained under the following condition:

$$R_1 = R_3 \Leftrightarrow \frac{\sin \varepsilon_2'}{\sin \varepsilon_3} = -\frac{\sin \varepsilon_2}{\sin \varepsilon_1}. \tag{17}$$

Analyzing formulas (4), (5), (9), (11), conclusion is made that the φ', ε_2', ε_2 and ε_1 angles depend on the ε_3, i.e., when choosing a certain value of the ε_3 angle, condition (17) is satisfied.

Value of the φ' angle in practice is less than 0.1 rad, and then equation (4) could be written in the form of an iterative expression:

$$\operatorname{tg} \varphi_n' = -\frac{\sin^3 \varepsilon_3}{\cos \varepsilon_3} + \operatorname{tg} \varepsilon_3 \cos 2\varepsilon_3 \operatorname{tg}^2 \varphi_{n-1}' - \frac{1 + 2\sin^2 \varepsilon_3}{2} \operatorname{tg}^3 \varphi_{n-1}' \tag{18}$$

at $\varphi_0' = 0$. Let us write expression (18) up to the fifth iteration order to obtain high calculation accuracy. Using the MathCAD mathematical software package [12], approximation will be as follows:

$$\varphi_1' = \operatorname{arctg}\left(-\frac{\sin^3 \varepsilon_3}{\cos \varepsilon_3} \right);$$

$$\varphi_2' = \operatorname{arctg}\left[-\frac{\sin^3 \varepsilon_3}{\cos \varepsilon_3} \left[1 - \frac{\sin^3 \varepsilon_3}{\cos \varepsilon_3} \left(\operatorname{tg} \varepsilon_3 \cos 2\varepsilon_3 + \frac{(1 + 2\sin^2 \varepsilon_3) \sin^3 \varepsilon_3}{2 \cos \varepsilon_3} \right) \right] \right]; \tag{19}$$

$$\varphi'_3 = \operatorname{arctg}\left(-\frac{\sin^3\varepsilon_3}{\cos\varepsilon_3} + \operatorname{tg}\varepsilon_3\cos 2\varepsilon_3\operatorname{tg}^2\varphi'_2 - \frac{1+2\sin^2\varepsilon_3}{2}\operatorname{tg}^3\varphi'_2\right);$$

$$\varphi'_4 = \operatorname{arctg}\left(-\frac{\sin^3\varepsilon_3}{\cos\varepsilon_3} + \operatorname{tg}\varepsilon_3\cos 2\varepsilon_3\operatorname{tg}^2\varphi'_3 - \frac{1+2\sin^2\varepsilon_3}{2}\operatorname{tg}^3\varphi'_3\right); \quad (19)$$

$$\varphi'_5 = \operatorname{arctg}\left(-\frac{\sin^3\varepsilon_3}{\cos\varepsilon_3} + \operatorname{tg}\varepsilon_3\cos 2\varepsilon_3\operatorname{tg}^2\varphi'_4 - \frac{1+2\sin^2\varepsilon_3}{2}\operatorname{tg}^3\varphi'_4\right).$$

Let us write formulas (5) and (9)–(11) taking into account (19):

$$\begin{gathered}\varepsilon'_2 = \varphi'_5 + 2\varepsilon_3;\\ \varepsilon_2 = k\,\lambda\,m - \sin\varepsilon'_2;\\ \varphi = \operatorname{arctg}\left(-\frac{\sin\varepsilon'_2\operatorname{tg}\varphi'_5}{\sin\varepsilon_2}\right);\\ \varepsilon_1 = \frac{\varphi-\varepsilon_2}{2}.\end{gathered} \quad (20)$$

Let us denote the left and the right sides of the equality in condition (17) as new functions of the ε_3 angle dependence; then, taking into account (20), the following is obtained:

$$f_1(\varepsilon_3) = \frac{\sin\varepsilon'_2}{\sin\varepsilon_3}; \quad (21)$$

$$f_2(\varepsilon_3) = \frac{-\sin\varepsilon_2}{\sin\varepsilon_1}. \quad (22)$$

Having solved the system of equations (21) and (22), let us find the ε_3 angle value. It should be noted that finding the absolute value analytically is tedious, so graphical solution is an easier way. The ε_3 angle value given in radians is the abscissa of the intersection point of the function graphs (21) and (22) shown in Fig. 4.

According to the data in Fig. 4, approximate value of the main beam incidence angle on the third surface (which is also the first) is: $\varepsilon_3 \approx 0.113528$ rad = = 6°30′17″. Function values for this argument are equal to: $f_1(0.113528)$ = = 1.9745402208; $f_2(0.113528)$ = 1.9745402332. The difference is observed only in the eighth decimal place. The φ'_5 angle value is: $\varphi'_5(0.113528)$ = = –0.0014629936.

Spectrometer representation (Table 2) was simulated in the Zemax automated analysis and optical systems design program. In accordance with it, the number of diffraction grating lines is set as m = 0.1 lines/μm.

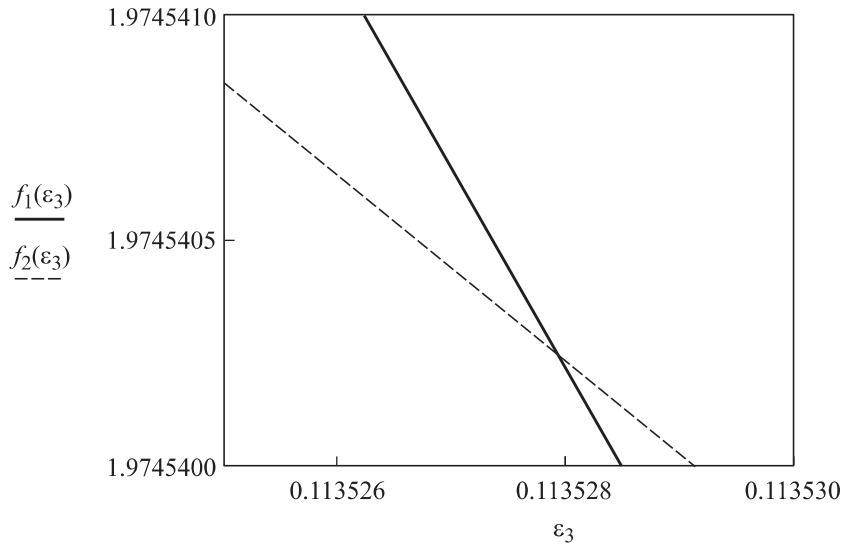

Fig. 4. Graphic determination of the main beam incidence angle on the third (first) surface

Table 2

Design parameters of the IR spectrometer

Surface	Radius R, mm	Thickness d, mm	Material
Object plane	∞	38.880	–
Concave mirror 1	–39.495	–19.491	Mirror
Aperture diaphragm. Diffraction grating	–20.000	–19.491	
Concave mirror 3 (1)	–39.495	–40.119	
Image plane	∞	–	–

It is necessary to estimate the confusion spot size over the entire width of the entrance slit corresponding to the line length of the selected radiation receiver. Its maximum line length in our case is 13.00 mm. Field split points in the sagittal section: –6.50 mm; –3.25 mm; 0; 3.25 and 6.50 mm. Object position $y = 9.5$ mm.

Radiation receiver transverse position is determined from the main beam tracing, it is equal to $y' = -6.944$ mm. Length of the resulting system is 40.12 mm, and the maximum mirrors' diameter is about 30 mm.

Let us demonstrate that the confusion spot size fits into the receiver matrix pixel size. Fig. 5 presents diagrams of the confusion spot for the fundamental wavelength (1.275 μm) at all field split points, as well as the corresponding values of the confusion spot radius root-mean-square values. The Airy disk (shown as a circle) for the fundamental wavelength in this case is 15.570 μm.

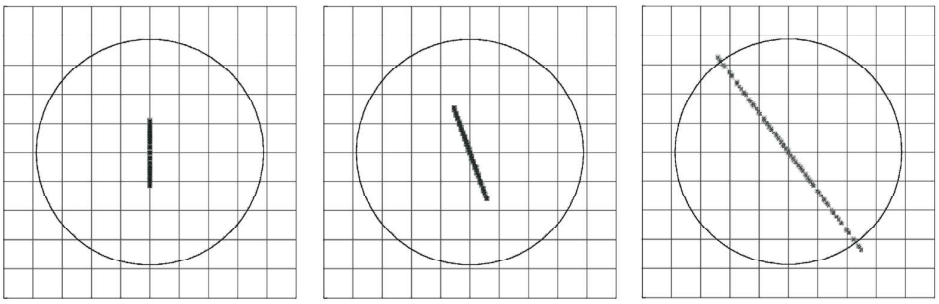

a *b* *c*

Fig. 5. Confusion spot points in the image plane for the wavelength of 1.275 μm: *a* are O (0; 9.500), I (0; –6.944 mm), RMSV-rad (2.417 μm); *b* are O (–3.250; 9.500), I (3.248 mm; –6.943 mm), RMSV-rad (3.614 μm); *c* are O (–6.500; 9.500), I (6.493 mm; –6.940 mm), RMSV-rad (8.897 μm); reference grid scale 40 μm

Data in Fig. 5 make it possible to determine the confusion spot size in the image plane: it is 2 · 8.9 μm. In this case, the receiver matrix pixel size is 20 μm. This means that the pixel is illuminated completely, there is no loss of the light signal, except due to diffraction phenomena, which satisfies the design assignment. Coma and astigmatism values for the maximum field are –0.00015 and 0.00786 mm.

Results obtained and discussion. The developed method for calculating the compact-size Offner spectrometer optical system is based on the Rowland circles and made it possible to calculate two optical schemes for the visible and the IR ranges. Calculation algorithm obtained from the condition of eliminating coma and astigmatism aberrations demonstrated its possibility to create compact optical systems with improved optical, technical and operational characteristics for promising and highly efficient Earth remote sensing optoelectronic equipment [13–15]. It was found that the confusion spot size of the simulated systems differs from the Airy disk size by not more than 2.5 μm, residual coma value for the maximum field is on the order of tenths of a micrometer, and residual astigmatism value is on the order of several micrometers.

Design solution optimization for the IR spectrum range made it possible to reduce the number of mirror surfaces in the optical system to two, which simplifies design and improves manufacturability. Simplicity, small overall dimensions, high optical characteristics and image quality of the Offner scheme in a wide spectral range close to the diffraction range were confirmed by simulating the developed optical schemes in the Zemax software program.

Effectiveness of the methodology is ensured by its simplicity and minimization of the computing resources in design and optimization of the design solutions.

Conclusion. A method for calculating a compact-size Offner spectrometer based on the Rowland circles was developed making it possible to optimize design solution based on the conditions of improving design, technological and optical characteristics. It is shown that theoretical assumptions of the promising capabilities of the Offner scheme underlying the study, i.e., simplicity, small overall dimensions and high optical characteristics in a wide spectral range, are confirmed by simulating the developed optical schemes in the Zemax program. Obtained algorithms, methods of optical systems calculation and design, on the one hand, reduce the development time, and on the other hand, increase quality of design.

Application of this method in the practice of calculating optical systems for the hyperspectral devices would make it possible to improve elemental base and precision optics technology up to a new higher level, which would contribute to creation of modern high-speed information-intensive tools for spectral analysis of the remote objects, including compact-size Earth remote sensing optoelectronic equipment.

Translated by K. Zykova

REFERENCES

[1] Arkhipov S.A., Zavarzin V.I., Senik B.N. Developing and fabricating optical systems for a prospective remote-earth-probe spacecraft. *J. Opt. Technol.*, 2013, vol. 80, no. 1, pp. 25–27. DOI: https://doi.org/10.1364/JOT.80.000025

[2] Prieto-Blanco X., Montero-Orille C., Couce B., et al. Analytical design of an Offner imaging spectrometer. *Opt. Express*, 2006, vol. 14, pp. 9156–9168. DOI: https://doi.org/10.1364/OE.14.009156

[3] Golovin A.D., Demin A.V. Simulation model of a multichannel Offner hyperspectrometer. *Komp'yuternaya optika* [Computer Optics], 2015, vol. 39, no. 4, pp. 521–528 (in Russ.). DOI: https://doi.org/10.18287/0134-2452-2015-39-4-521-528

[4] Kazanskiy N.L., Kharitonov S.I., Doskolovich L.L., et al. Modeling the performance of a spaceborne hyperspectrometer based on the Offner scheme. *Komp'yuternaya optika* [Computer Optics], 2015, vol. 39, no. 1, pp. 70–76 (in Russ.). DOI: https://doi.org/10.18287/0134-2452-2015-39-1-70-76

[5] Gorbunov G.G., Demin A.V., Nikiforov V.O., et al. Hyperspectral apparatus for remote probing of the Earth. *J. Opt. Technol.*, 2009, vol. 76, no. 10, pp. 651–656. DOI: https://doi.org/10.1364/JOT.76.000651

[6] Kim S.H., Kwo D., Lawrence G., et al. Design and construction of an Offner spectrometer based on geometrical analysis of ring fields. *Rev. Sc. Instrum.*, 2014, vol. 85, no. 8, art. 083108. DOI: https://doi.org/10.1063/1.4892479

[7] Mouroulis P., Green R.O., Chrien T.G. Design of pushbroom imaging spectrometers for optimum recovery of spectroscopic and spatial information. *Appl. Opt.*, 2000, vol. 39, no. 13, pp. 2210–2220. DOI: https://doi.org/10.1364/AO.39.002210

[8] Zavarzin V.I., Li A.V. Calculation of the centered reflecting objective with eccentrically located image field. *Herald of the Bauman Moscow State Technical University, Series Instrument Engineering*, 2016, no. 2 (107), pp. 103–116 (in Russ.).
DOI: http://doi.org/10.18698/0236-3933-2016-2-103-116

[9] Zemax 13 — PO dlya analiza i proektirovaniya opticheskikh system [Zemax 13 — software for designing optical systems]. Available at: https://www.zemax.com (accessed: 16.08.2021).

[10] Arkhipov S.A., Zavarzin V.I., Malykhin V.A., et al. Alignment and calibration of long-focus three-mirror lens with eccentric position of image field. *Herald of the Bauman Moscow State Technical University, Series Instrument Engineering*, 2009, no. 4 (77), pp. 24–36 (in Russ.).

[11] Zavarzin V.I., Li A.V. Quality control of large-scale mirror objectives with eccentric image field. *Herald of the Bauman Moscow State Technical University, Series Instrument Engineering*, 2014, no. 6 (99), pp. 39–48 (in Russ.).
DOI: http://doi.org/10.18698/0236-3933-2014-6-39-48

[12] PTC MathCAD Prime 7 — matematicheskoe PO dlya inzhenernykh raschetov [PTC MathCAD Prime 7 — math software for engineering computations] (in Russ.). Available at: https://www.mathcad.com/ru (accessed: 16.08.2021).

[13] Sellar R.G., Boreman G.D. Comparison of relative signal-to-noise ratios of different classes of imaging spectrometers. *Appl. Opt*., 2005, vol. 44, no. 9, pp. 1614–1624.
DOI: https://doi.org/10.1364/AO.44.001614

[14] Offner A., Decker W.B. An f.1.0 Camera for astronomical spectroscopy. *J. Opt. Soc. Am*., 1951, vol. 41, no. 3, pp. 169–172. DOI: https://doi.org/10.1364/JOSA.41.000169

[15] Mouroulis P., Wilson D.W., Maker P.D., et al. Convex grating types for concentric imaging spectrometers. *Appl. Opt*., 1998, vol. 37, no. 31, pp. 7200–7208.
DOI: https://doi.org/10.1364/ao.37.007200

Zavarzin V.I. — Dr. Sc. (Eng.), Professor, Department of Laser and Optoelectronic Systems, Dean of the Department of Optoelectronic Instrument Engineering, Bauman Moscow State Technical University (2-ya Baumanskaya ul. 5, str. 1, Moscow, 105005 Russian Federation).

Zaitsev I.M. — Student, Department of Laser and Optoelectronic Systems, Bauman Moscow State Technical University (2-ya Baumanskaya ul. 5, str. 1, Moscow, 105005 Russian Federation).

Yakubovskiy S.V. — Student, Department of Laser and Optoelectronic Systems, Bauman Moscow State Technical University (2-ya Baumanskaya ul. 5, str. 1, Moscow, 105005 Russian Federation).

Please cite this article as:

Zavarzin V.I., Zaitsev I.M., Yakubovskiy S.V. Method for calculating the Offner compact-size spectrometer. *Herald of the Bauman Moscow State Technical University, Series Instrument Engineering*, 2021, no. 4 (137), pp. 139–151.
DOI: https://doi.org/10.18698/0236-3933-2021-4-139-151